Ultrafast Infrared Studies of the Reaction Mechanism of Silicon−Hydrogen Bond Activation by η^5-CpV(CO)$_4$

Preston T. Snee, Haw Yang, Kenneth T. Kotz, Christine K. Payne, and Charles B. Harris*

Department of Chemistry, University of California, Berkeley, California, 94720 and Chemical Sciences Division, Ernest Orlando Lawrence Berkeley National Laboratory, Berkeley, California, 94720

Received: June 15, 1999; In Final Form: October 1, 1999

The photochemical Si−H bond activation reaction by the group VB, d^4 organometallic compound η^5-CpV(CO)$_4$ (Cp = C_5H_5) has been studied in neat triethylsilane under ambient conditions. The spectral evolutions of the metal-bonded CO stretching bands were monitored from 300 fs to 800 ps following UV photolysis using femtosecond pump−probe spectroscopic methods. The reactive intermediates observed on the ultrafast time scale were also studied using density functional theory as well as ab initio quantum chemical modeling. It was found that photolysis of vanadium tetracarbonyl resulted in the formation of tricarbonyls in either the singlet or triplet electronic state following CO loss. The subsequent reaction was partitioned into two pathways by the initial solvation of the tricarbonyls through the Si−H bond or an ethyl group of the solvent molecule. Knowledge of the elementary reaction steps including changes in molecular morphology and electronic multiplicity allowed a comprehensive description of the chemical reactivity.

I. Introduction

The photochemical oxidative addition of a Si−H bond to certain transition metal complexes has been the focus of many research efforts since its initial discovery by Jetz and Graham in 1971.[1] This type of bond activation reaction is critical in hydrosilylation processes and provides a comparison to oxidative addition reactions by other organometallic complexes.[2−5] We have recently reported our initial findings of the Si−H bond activation reaction of Et_3SiH (Et = C_2H_5) with the group VIIB, d^6 organometallic compound η^5-CpMn(CO)$_3$ (Cp = C_5H_5).[6] Later a comprehensive study of Si−H bond activation of Et_3-SiH by η^5-CpM(CO)$_3$ (M = Mn, Re) was published,[7] hereafter referred to as paper I. To extend our knowledge of Si−H activation, we have studied the photochemical activation of Si−H bonds using the d^4 organometallic compound η^5-CpV(CO)$_4$ in neat triethylsilane.

There are relatively few studies of silane Si−H bond activation by group VB organometallics, and as such, their reactivities have not been well characterized. George et al. have shown that the photolysis of η^5-CpV(CO)$_4$ in the presence of Et_3SiH results in the arrested oxidative addition product η^5-CpV(CO)$_3$(η^2-HSiEt_3).[8] Thus, the coordinated triethylsilane molecule acts as a σ-donor ligand and some residual Si−H interaction remains in the final product.[5,9] Rest and Hitam have proposed that a coordinatively unsaturated, 16-e$^-$ η^5-CpV(CO)$_3$ photoproduct is formed upon UV irradiation of η^5-CpV(CO)$_4$ in low-temperature matrices (Scheme 1).[10,11] Substitution studies of η^5-CpV(CO)$_4$ under ambient conditions suggest that the tricarbonyl species coordinates to the solvent to form η^5-CpV(CO)$_3$(solvent), which then reacts with an entering ligand.[12−16] There have been no studies, however, of the early time dynamics of the reaction mechanism due to the extremely fast reaction rates.

The paper is organized as follows: The experimental methods and calculation procedures are described in section II. The results and detailed data analysis are presented in section III. Implications of the results are discussed in section IV. In particular, we discuss the nature of the observed transient intermediates and their interaction with solvent. A comprehensive reaction mechanism is described in the end of section IV.

SCHEME 1

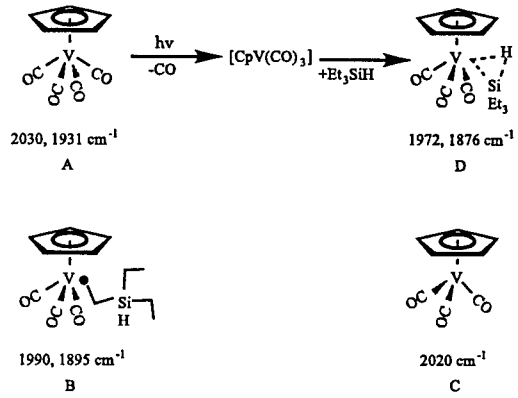

II. Methods

Sample Handling. The compound η^5-CpV(CO)$_4$ (97%, **A**) was purchased from Strem, Inc. and used without further purification. Anhydrous heptane (99%) was purchased from Aldrich. To ensure that moisture and oxygen did not interfere with the experiment, the triethylsilane acquired from Gelest, Inc., was dried in an alumina column and distilled under nitrogen. All samples were prepared under nitrogen atmosphere in an airtight, liquid IR flow cell (Harrick Scientific Corporation). The concentration of the η^5-CpV(CO)$_4$/Et_3SiH solution was approximately 7 mM. The absorbance of a 125 μm thick sample of this concentration at 295 nm was about 0.7 OD.

Femtosecond Infrared Spectroscopy. Details of the femtosecond IR (fs-IR) spectrometer setup have been published elsewhere.[17] In brief, the output of a Ti:sapphire oscillator was

* To whom correspondence should be addressed. Phone: (510) 642-2814. FAX: (510) 642-6724. E-mail address: harris@socrates.berkeley.edu

10.1021/jp991964j CCC: $18.00
Published on Web 11/10/1999

amplified in two prism-bored dye-cell amplifiers,[18] which were pumped by the output of a frequency-doubled 30 Hz Nd:YAG laser. The amplified light centered at ~810 nm was then split into three beams. One beam was further amplified to give 70 fs, 20 μJ pulses. The other two beams were focused into two sapphire windows to generate white light continuum. Desired wavelengths of the white light were selected by two band-pass (BP) filters with a full-width at half-maximum (fwhm) of 10 nm and further amplified by three-stage dye amplifiers to produce light pulses centered at 590 and 690 nm. In this study, the excitation pulse of 295 nm was generated by frequency doubling the 590 nm pulses. The resulting UV photons (with energy of ~6 μJ/pulse) were focused to a spot of ~200 μm diameter at the sample to initiate the chemical reactions. The required time delay between a pump pulse and a probe pulse was achieved by guiding the 590 nm pump beam through a variable delay line before being frequency doubled.

The broadband, ultrafast probe pulses centered at ~5 μm were generated by mixing the 690 nm beam with the 810 nm beam. The resulting ~5 μJ IR pulses having temporal fwhm of about 70 fs and spectral bandwidth of about 200 cm^{-1} were split into a signal and a reference beam. Both the signal beam and the reference beam were then focused into an astigmatism-corrected spectrographic monochromator (Spectra-Pro-150, Acton Research Corp., 150 gv/mm, 4.0 μm blazed) to form two spectrally resolved images on a focal-plane-array (FPA) detector. The two frequency-resolved images were digitized by two windows of 12 × 200 pixels, which allowed simultaneous normalization of a 70 cm^{-1} spectrum. The sensoring chip of the detector was an engineer grade, 256 × 256-element HgCdTe (MCT) matrix of dimensions 1.28 × 1.28 cm (Raytheon Amber Co.). The typical spectral and temporal resolutions for this setup are 4 cm^{-1} and 300 fs, respectively. The polarizations of the pump and the probe pulse were set at the magic angle (54.7°) to ensure that all signals were due to population dynamics. A broad, wavelength independent background signal from CaF_2 windows has been subtracted from the transient spectra and kinetic traces.

Quantum Chemical Modeling. Density functional theory (DFT) and ab initio modeling provide a means by which to study the nature of possible candidates for the observed reactive intermediates whose lifetimes are too short for conventional characterization. We used Becke's three-parameter hybrid functional[19] for the exchange-correlation energy combined with the Lee−Yang−Parr correlation functional,[20] denoted B3LYP.[21] All geometry optimizations were followed by a frequency calculation to make certain that the optimized geometry was at a minimum. The basis set consisted of the 6-31G** basis functions for H, C, O, and Si,[22,23] and the 10-electron Los Alamos Effective Core Potential (ECP) for V with the outermost core orbitals included in the valence description.[24] This basis set will be referred to as LACVP** later in the text. The Jaguar package was used for the DFT calculations.[25] Ab initio calculations were carried out using the DFT optimized geometries to the MP2 level of theory for closed shell species and UMP2 for closed shell species. These MP2 calculations were carried out using the GAMESS-US package.[26]

To determine the possible involvement of a ring-slipped η^3-$CpV(CO)_4$ intermediate, we have also performed a geometry optimization for η^3-$C_3H_5V(CO)_4$ as a model. We then calculated the natural bond orbital (NBO) charge density,[27] as well as a frequency analysis of this structure to aid in the assignment of the observed intermediate species.

To better assess the energy splitting between the unsolvated singlet and triplet species, the complete active space multiconfigurational self-consistent field (CAS-MCSCF) followed by second-order many particle perturbation treatment (PT2) was carried out using the DFT geometries. Because of the high computational demand, the lanl2dz basis set was used for these calculations.[24,28−30] The restricted open-shell Hartree−Fock wave functions were calculated as the starting orbitals for subsequent CAS-MCSCF calculations. During the CAS-MCSCF calculation for the triplet species, five occupied d-type orbitals and five d-type virtual orbitals were correlated; the corresponding 10 d-type orbitals were correlated in the singlet calculation. The CAS-MCSCF wave functions were then used for the second-order perturbation method of Nakano implemented into GAMESS-US.[31]

To represent the intermediates in a practically tractable way, the complexation of the ethyl moiety of Et_3SiH with the metal fragment η^5-$CpV(CO)_3$ was modeled by an ethane/η^5-$CpV(CO)_3$ complex. The final product η^5-$CpV(CO)_3(HSiEt_3)$ was modeled by η^5-$CpV(CO)_3(HSiH_2CH_3)$. Symmetry was imposed for the singlet and triplet tricarbonyl species as well as on ligands for counterpoise calculations (η^5-$CpV(CO)_3$, C_s; CO, C_{2v}; C_2H_6, D_{3d}; SiH_2CH_3, C_{3v}). All other structures were optimized without constraints. The geometries of these structures are given in the supplemental information section.

The metal−ligand interaction energies were calculated as the energy difference between the products and the reactant in the reaction

$$\eta^5\text{-}CpV(CO)_3L \rightarrow \eta^5\text{-}CpV(CO)_3 + L$$

where L could be CO, C_2H_6, or $HSiH_2CH_3$. The basis set superposition error (BSSE)[32] correction was calculated using a fragment relaxation procedure recently proposed by Xantheas,[33] which gives correct results at the complete basis set limit. All the zero point energy (ZPE) corrections to the complexation energies were calculated from vibrational frequencies at the DFT/B3LYP level.

The frequency analyses for the ethane-solvated complex and triplet species are also used in the assignment of species F and C in section IV.

III. Results

The infrared spectra in the CO stretching region are presented in a form of difference absorbance in which positive bands indicate the appearance of new species while negative bands (bleaches) represent the depletion of parent molecules.

A. Photolysis of η^5-$CpV(CO)_4$ in Heptane. The photolysis of η^5-$CpV(CO)_4$ in heptane was studied in order to provide a basis for comparison to the triethylsilane data. Shown in Figure 1 are the femtosecond-IR difference spectra of η^5-$CpV(CO)_4$ in neat heptane following excitation at 295 nm. There are three broad positive peaks appearing in the spectra at 10 ps, which narrow at later times. This process is indicative of vibrational cooling of the CO ligands.[34−36] On the basis of previous room-temperature studies,[8] and wavelength-dependent photolysis experiments in matrix isolation studies,[10] the bands at 1895 and 1990 cm^{-1} are assigned to a solvated singlet η^5-$CpV(CO)_3$-(heptane) photoproduct E. (Note that different species notations are used to differentiate between the alkane and triethylsilane studies.) The third peak at 2020 cm^{-1} is an unknown intermediate, denoted F. The assignment of this species will be discussed in section IV. Shown in Figure 2 are the kinetic traces of the alkyl solvated singlet η^5-$CpV(CO)_3$(heptane) and intermediate F. Species F shows a fast 6.3 ± 1.9 ps rise followed by a biexponential decay of 50 ± 10 ps and a much longer time

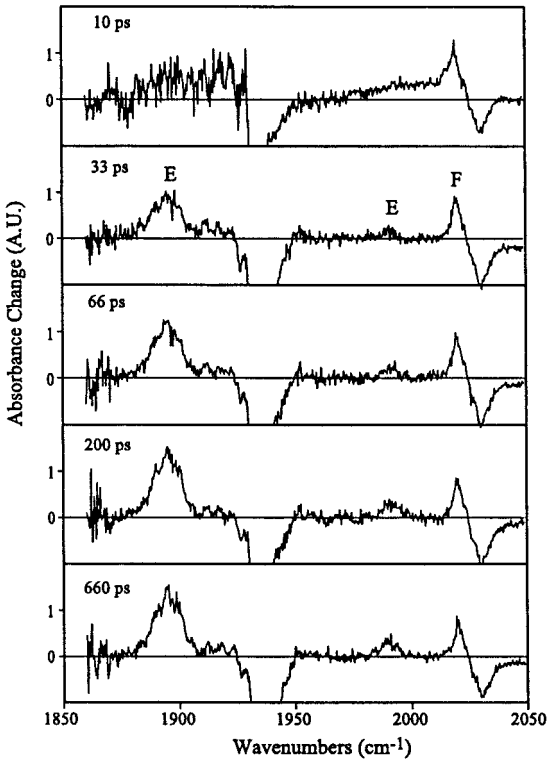

Figure 1. Transient difference spectra in the CO stretching region for η^5-CpV(CO)$_4$ in neat heptane at 10, 33, 66, 200, and 660 ps following 295 nm UV photolysis (AU = arbitrary units ~ 1 mOD).

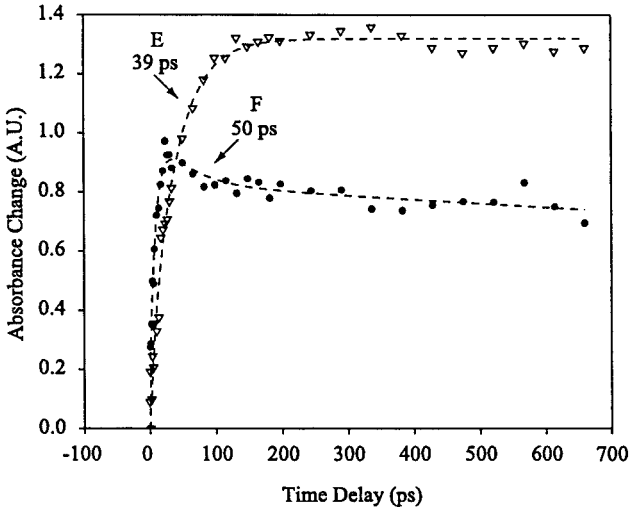

Figure 2. Ultrafast kinetics of η^5-CpV(CO)$_4$ in neat heptane after 295 nm UV photolysis at 1892 cm^{-1}, the CO stretch of the alkane adduct η^5-CpV(CO)$_3$ (open triangles) (E), and at 2020 cm^{-1} (filled circles), the CO stretch of the triplet tricarbonyl (F). The time constants for the exponential fits (dashed lines) are shown in the graph (AU = arbitrary units).

component (≫1 ns), which cannot be accurately determined within the limitations of our spectrometer.[37] The 50 ps decay of species F represents the loss of a small portion (~15%) of the total amount formed. It can be seen that the singlet solvated tricarbonyl E displays a biexponential formation with time constants of 6.6 ± 5.7 and 39 ± 3 ps, respectively. The rise times of these species are most likely due to vibrational cooling of the initially hot photoproducts, although the fast initial rise times are difficult to calculate accurately due to the presence of hot and combination bands. These data are used in the comparison of the reactivity of these species in triethylsilane in section IV.

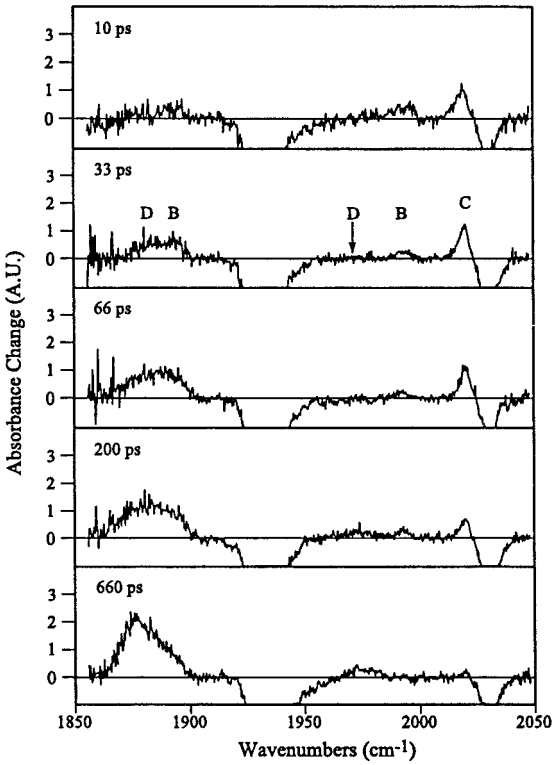

Figure 3. Transient difference spectra in the CO stretching region for η^5-CpV(CO)$_4$ in neat triethylsilane at 10, 33, 66, 200, and 660 ps following 295 nm UV photolysis. Under the experimental conditions, the large cross section of the solvent Si−H band (~2100 cm^{-1}) and the parent CO band (1931 cm^{-1}) make it difficult to access some regions of the spectrum (AU = arbitrary units).

B. Activation of the Silicon−Hydrogen Bond of Et$_3$SiH by η^5-CpV(CO)$_4$ Shown in Figure 3 are the femtosecond-IR spectra of η^5-CpV(CO)$_4$ in neat Et$_3$SiH following excitation at 295 nm. The peaks at 1876 and 1973 cm^{-1} are assigned to the product η^5-CpV(CO)$_3$(HSiEt$_3$), denoted D (Scheme 1).[8] The peaks at 1895 and 1990 cm^{-1} are attributed to species B, formed from the solvation of singlet η^5-CpV(CO)$_3$ (B*) through the ethyl moiety of Et$_3$SiH. These bands are highly overlapped and, as such, Gaussian fits to the data were used to decouple these absorbances. Kinetic traces were then created by plotting the peak height from our fits over time. Unfortunately, this results in larger errors for the kinetic traces. The band appearing at 2020 cm^{-1} is attributed to an unknown intermediate, denoted C. Shown in Figure 4 are the kinetic traces of B, C, and the final product D following 295 nm excitation. The kinetics of C recorded at 2020 cm^{-1} exhibit a fast 8.8 ± 0.3 ps rise followed by a 360 ± 10 ps decay. There does not appear to be a fast decay component to the intermediate C as was observed in heptane; however, this decay component would be obscured as C appears to react quickly with triethylsilane (see below). Further, the 50 ps decay seen in the heptane data accounted for the loss of no more than 15% of the total intermediate formed, while the intermediate seems to react completely away in triethylsilane. The ethyl-solvated singlet B displays kinetic behavior similar to that of the triplet species, with a rise time of 36 ± 6 ps followed by a 470 ± 75 ps decay. The product band of D at 1876 cm^{-1} displays a biexponential rise of 55 ± 6 ps and 350 ± 140 ps. Within the limitations of our instrumentation, the decay of the intermediates B and C are most likely correlated to the formation of the final product D, as the parent bleach does not recover on this time scale.[38] As

TABLE 1: Critical Bond Distances (Å) on the Important Structures for the Si−H Bond Activation Reactions Optimized at the DFT/B3LYP Level of Theory

compound	Cp−M	M−CO	C−O	M−H	M−Si(C)	Si−H (C−H)
η^5-CpV(CO)$_4$	1.94 [1.94][a]	1.94 [1.94][a]	1.16 [1.13][a]			
Singlet η^5-CpV(CO)$_3$	1.93	1.95 (1.93)[b]	1.16 (1.16)[b]			
Triplet η^5-CpV(CO)$_3$	1.95	1.98 (1.95)[b]	1.15 (1.16)[b]			
η^5-CpV(CO)$_3$(H$_3$CCH$_3$)	1.94	1.94 (1.92)[b]	1.16 (1.16)[b]	2.24	3.20	1.11
η^5-CpV(CO)$_3$(HSiH$_2$CH$_3$)	1.94	1.93, 1.94 (1.92)[b]	1.16 (1.16)[b]	1.85	3.11	1.53

[a] Numbers in brackets are experimental values from: Almond, M. J.; Page, E. M.; Rice, D. A.; Hagen, K. *J. Organomet. Chem.* **1996**, *511*, 303. [b] Numbers in parentheses are for the nonequivalent CO ligand (there are two equivalent and one nonequivalent ligand due to the mirror symmetry of the species; see Figure 5).

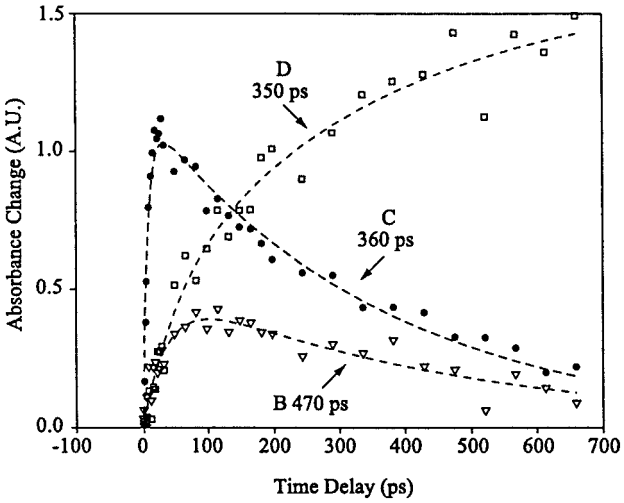

Figure 4. Ultrafast kinetics of η^5-CpV(CO)$_4$ in neat triethylsilane after 295 nm UV photolysis at 1895 cm^{-1}, the CO stretch of the alkane adduct η^5-CpV(CO)$_3$ (open triangles) (B), at 2020 cm^{-1} (filled circles), the CO stretch of the triplet tricarbonyl (C), and at 1876 cm^{-1} (open squares), the final product (D). The time constants for the exponential fits (dashed lines) are shown in the graph (AU = arbitrary units).

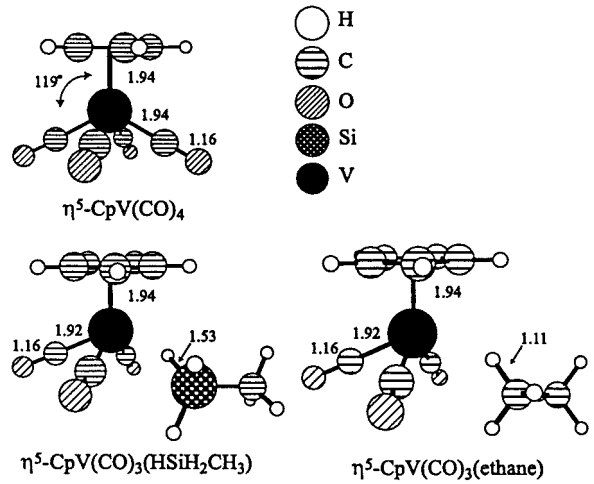

Figure 5. Geometries of the parent molecules, the ethane solvate, and the final product optimized at the DFT/B3LYP level of theory. The bond lengths are in Å, and angles, in degrees.

in the heptane data, the early rise times may be attributed to vibrational cooling of the photoproducts.

Finally, the free-energy barrier of the process from B → D and C → D can be derived from the kinetic traces. If one assumes a simple transition-state theory, the reaction rate can be expressed as the reciprocal of the observed lifetime τ,

$$\text{reaction rate} \approx (1/\tau) = (kT/h)e^{-\Delta G^*/kT}$$

where k is the Boltzmann constant, h is Plank's constant, T is room temperature (298.15 K), and ΔG^* is the free energy of activation. The reaction barriers, estimated from the intermediate decay times, are $\Delta G^* = 4.72 \pm 0.08$ kcal/mol for the ethyl solvate B → D channel and $\Delta G^* = 4.57 \pm 0.02$ kcal/mol for the intermediate C → D channel.

C. DFT and ab Initio Calculation Results. *Geometry Optimization.* Figure 5 shows the geometries of the parent molecule η^5-CpV(CO)$_4$, the singlet metal tricarbonyl solvated by an ethane molecule η^5-CpV(CO)$_3$(ethane), and the final product η^5-CpV(CO$_3$)(HSiH$_2$CH$_3$);[39] all optimized at the DFT/B3LYP level of theory. As displayed in Table 1, the metal−Cp and metal−CO distances for the parent molecule agree reasonably well with the gas-phase experimental values,[40] except for the slightly overestimated C−O bond lengths. The geometric parameters for all CO ligands are given.

For the ethane tricarbonyl complex in Figure 5, the ethane molecule interacts with the metal center by one of its C−H bonds via an η^2 interaction. The bond length for the coupled C−H bond is 1.11 Å, which is extended by +0.02 Å compared to 1.09 Å for the C−H bond of a free ethane molecule from the same level of calculation. This suggests that the V atom interacts weakly with a C−H bond.[41] Finally, the extent of the Si−H bond activation is demonstrated by the Si−H bond distance in the final product. The calculated Si−H bond length for the metal complex is 1.53 Å compared with the monomer silane Si−H bond length of 1.49 Å. Thus, there is a net increase of 0.04 Å, which is slight compared to the Si−H bond lengthening of ∼1.3 Å in the fully activated species (CO)$_2$(dppe)Fe(HSiMe$_3$).[42]

Shown in Figure 6 are the geometries for the 16-e$^-$ species η^5-CpV(CO)$_3$ in its (unsolvated) singlet and triplet states. The relevant structural parameters are given for both the two equivalent carbonyl ligands (due to mirror-plane symmetry) and the one nonequivalent carbonyl ligand. Despite the overall similarity of the singlet and triplet species, one notices a difference in the OC−M−CO angle. For example, the angle between the OC$_{eq}$−M−CO$_{non-eq}$ bond increases from 80° in the singlet to 92° in the triplet state. Projected into the plane of the cyclopentadienyl ring, the triplet species has the carbonyl ligands arranged in a more trigonal fashion, while the singlet state is less symmetric. In addition, the V−Cp and M−CO distances are longer in the triplet species than in the singlet, and the equivalent CO bond lengths are shorter in the triplet compared to the singlet. Such a decrease in the metal−CO interaction in the triplet state has also been observed in calculations of η^5-CpM(CO) (M = Co, Rh, and Ir)[43] and η^5-Cp*W(NO)(CO),[44] as well as our own calculation of η^5-CpM(CO)$_2$ (M = Mn and Re) in paper I.

Energy Calculations. The calculated metal−ligand interaction energies are listed in Table 2. All binding energies have been calculated at the DFT/B3LYP and MP2 levels of theory using the DFT geometries. The calculation of the ethane complex is likely to underestimate the true alkyl-solvated species complex-

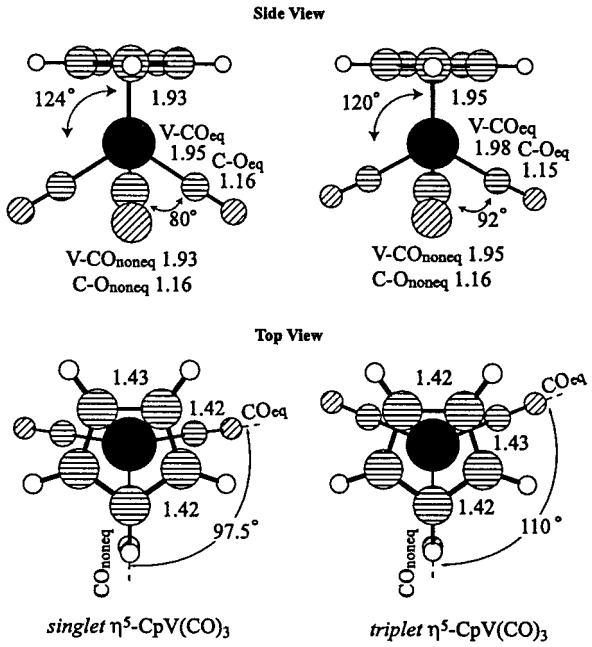

Figure 6. Side view and top view for the DFT/B3LYP optimized geometries of the 16-e$^-$ species. The bond lengths are in Å, and angles, in degrees.

TABLE 2: Calculated Binding Energies (kcal/mol) for Singlet η^5-CpV(CO)$_3$L

	DFT			MP2[a]		
L	ZPE[b]	ΔE	ΔE (BSSE)	ZPE[b]	ΔE	ΔE (BSSE)
CO	−2.89	37.55	30.78	−2.89	55.64	42.14
Et	−0.97	1.99	0.26	−0.97	9.17	4.38
SiH_3CH_3	−1.64	8.12	5.63	−1.64	23.35	15.27

[a] Calculated using DFT optimized geometries. [b] Calculated using DFT/B3LYP frequency analysis at 298.15 K.

TABLE 3: Comparison of the Energy Difference, ΔE = E(singlet) − E(triplet) (kcal/mol), between Singlet and Triplet η^5-CpV(CO)$_3$ Calculated Using Different Methods[a]

	ΔE
HF[b]	32.38
UMP2[b]	−23.79
DFT[b]	3.10
CAS-MCSCF[c]	2.39
CAS-MCSCF-PT2[c]	7.28

[a] Calculated using DFT optimized geometries. [b] LACVP** basis set was used. [c] LANL2DZ basis set was used.

ation energy due to the fact that the interaction energy between a transition metal and a series of chain alkanes may increase with chain length.[45−47] Nonetheless, the calculated binding energy of the ethane allows a qualitative understanding of the relative stability of η^5-CpV(CO)$_3$(alkane). Our MP2 results show that the complexation energy is 4.38 kcal/mol for the ethane complex and 15.27 kcal/mol for the silane complex, while our DFT results predict much weaker interactions.

In the single point calculations of (unsolvated) singlet and triplet η^5-CpV(CO)$_3$, the DFT and CAS MCSCF-PT2 results predict a lower energy for the triplet state relative to that of the singlet by ΔE = 3.10 and 7.28 kcal/mol, respectively. The UMP2 calculations, on the other hand, show that the singlet is lower in energy by 23.8 kcal/mol. The inconsistency may be due to spin contamination of the UMP2 wave function, which had a $\langle S^2 \rangle$ value of 2.5. The results are summarized in Table 3.

The numerical CO stretching frequencies at the DFT level were calculated for the singlet η^5-CpV(CO)$_3$(ethane) (2021 and 2086 cm^{-1}) and for the triplet η^5-CpV(CO)$_3$ (2039 and 2113 cm^{-1}) as well as for the parent η^5-CpV(CO)$_4$ (2044 and 2115 cm^{-1}). We have also calculated the CO stretching frequencies for the model ring-slipped structure η^3-C_3H_5V(CO)$_4$ (2025, 2049, 2057, and 2115 cm^{-1}). The NBO charge density of the parent metal center (−1.02e) as well as for η^3-C_3H_5V(CO)$_4$ (−0.74e) was calculated. These results will be used in the assignment of F and C in the next section.

IV. Discussion

A. Photolysis of η^5-CpV(CO)$_4$ in Heptane. The transient intermediate F observed at 2020 cm^{-1} has been proposed as a ring-slipped η^3-CpV(CO)$_4$.[10] This assignment was based upon analogous spectral CO peak shifts seen in other iron-based organometallic species that undergo partial dechelation of a hydrocarbon ring coordinated to the metal. In the latter case, however, the differences in the metal center and coordinating ligand compared to the CpV(CO)$_4$ system make these analogies inconclusive. This assignment does not fit our experimental results as well. For one, the fast decay of 50 ± 10 ps in the population of F appears to be accompanied by the formation of the solvated singlet η^5-CpV(CO)$_3$, which has a growth component of 39 ± 3 ps. There parent bleach signal, which was monitored at 2030 cm^{-1}, does not show a corresponding recovery on this time scale, which would indicate that the decay of F results in the regeneration of the parent molecule. The reactivity of this species is also very different in triethylsilane. Because of these considerations, it is unlikely that species F is ring-slipped η^3-CpV(CO)$_4$.

Another possibility is that the unknown photoproduct F is a tricarbonyl in another electronic spin state, most likely a triplet species. The existence of stable paramagnetic complexes, such as η^5-CpV^{I}(ethylene)(PMe$_3$)$_2$ and η^5-CpV^{III}Cl$_2$(PMe)$_2$, confirms that organometallic vanadium 16-e$^-$ complexes may adopt a high-spin electronic structure.[48,49] As such, we have carried out DFT and ab initio calculation on (unsolvated) triplet and singlet η^5-CpV(CO)$_3$. Although the UMP2 results suggest a singlet ground state, both the DFT and CAS MCSCF-PT2 calculations predict a triplet ground state for η^5-CpV(CO)$_3$. Further, as DFT frequency calculations are known to be accurate enough to be of predictive value,[50−52] we have calculated the CO stretching frequencies for the triplet, model ring-slipped, and ethyl-solvated singlet states. Unfortunately, the results were inconclusive. The DFT calculations for the triplet tricarbonyl show a +27 cm^{-1} shift with respect to the higher-energy CO band of the solvated singlet species, which is comparable with experimental observation of a +30 cm^{-1} shift of F with respect to E. The other calculated triplet carbonyl stretch is only 5 cm^{-1} red shifted from the parent absorption. These calculations, as well as the low-temperature matrix study, suggest that a second triplet absorption is masked by the parent bleach in our data.[53] On the other hand, the model ring-slipped species shows a high-frequency blue shift similar to that of the calculated triplet. The other three bands might be obscured by parent bleach and solvated singlet peaks in the experimental data as well as in the previous matrix experiments. Consequently, a ring-slipped intermediate may not be ruled out from the spectral data alone. Despite the inconclusive frequency analysis, based upon the kinetic data as well as the fact that triplet η^5-CpV(CO)$_3$ appears to be the ground state, it is unlikely that F is a ring-slipped 16-e$^-$ species and it is reasonable to attribute this intermediate to a triplet state of η^5-CpV(CO) $_3$.

B. Activation of the Silicon−Hydrogen Bond of Et_3SiH by η^5-CpV(CO)$_4$. *Comparison with Previous Work.* In our

previous study it was found that η^5-CpM(CO)$_3$ (M = Mn, Re) formed coordinately unsaturated 16 e$^-$ dicarbonyl species via CO loss upon photolysis. For the Re complex, the reaction coordinate was divided into two distinct channels by the initial solvation: formation of an ethyl-solvated moiety via solvation of the ethyl group and activation of the Si−H bond via Si−H solvation. The ethyl solvate decayed into the final bond-activated product via a dissociative mechanism on a microsecond time scale. The Mn complex mechanism was similar except for the formation of an electronic triplet state intermediate, the decay of which was partitioned between formation of the singlet ethyl solvate and of the final product in a concerted spin crossover/Si−H solvation. The present study provides a basis for comparison to the previous data, especially concerning the reactivity of the proposed triplet state.

Formation and Solvation of the Triplet and Singlet Intermediates in Triethylsilane. After excitation at 295 nm in neat triethylsilane, the parent molecule η^5-CpV(CO)$_4$ quickly loses one CO ligand to produce two tricarbonyls (designated as B and C). On the basis of the similarities of the peak positions in the ultrafast heptane spectra, the intermediate B is assigned as a singlet ethyl solvate and C is the triplet tricarbonyl. These species decay on a hundreds of picoseconds time scale to form the final product D.

There are a few important differences between the dynamics of the photogenerated intermediates in different solvents. First of all, note the increase in triplet/singlet population ratio in triethylsilane compared to that in heptane. This is suggestive of either a fast depletion of the singlet species at early times in triethylsilane or a change in the branching ratio between triplet and singlet formation in the different solvents. Unfortunately, the early time dynamics of this system are obscured by vibrational relaxation, and as such, it is difficult to differentiate between these two possibilities.

In the context of C being a triplet state η^5-CpV(CO)$_3$, we next discuss the interaction of C and the solvent. It has been suggested theoretically that transition metals in their triplet state interact only weakly with alkane solvents,[54−56] which has been used to explain the high reactivity of triplet η^5-CpCo(CO) toward a free CO in liquefied rare-gas solution or in alkane solution.[57] It was found by Dougherty and Heilweil that triplet η^5-CpCo(CO) reacts with the strongly binding ligand 1-hexene to form presumably a singlet π-complex within picoseconds,[58] while a lifetime of ∼milliseconds of triplet η^5-CpCo(CO) was observed in weakly binding solvents such as Kr and Xe.[57] Hence strongly interacting solvent molecules need to be considered in describing the reaction coordinate for spin crossover and solvent exchange. A similar argument was used in paper I for the loss of triplet η^5-CpMn(CO)$_2$ observed in triethylsilane solution. It would appear that a triplet transition metal complex is preferentially solvated by the more strongly coupling sites of a solvent molecule. On the basis of the arguments above, our data suggest that the triplet species, which for the most part is long-lived in a nonreactive alkane solvent, is quickly depleted directly via a concerted spin crossover/solvation through Si−H bond of the solvent molecule.

It appears that the solvation and reaction dynamics of the singlet species are different from that of the triplet. Upon photolysis, the uncoordinated singlet η^5-CpV(CO)$_3$ (B*) species is quickly solvated by the ethyl moiety of Et$_3$SiH to form B. This adduct then decays to form the product D on a time scale of 470 ± 75 ps. One can imagine several mechanisms to explain this formation of the final product. First of all, the solvent molecule may undergo a dissociation followed by a rotation and recoordination to form the final product, perhaps assisted by an associating solvent molecule that lowers the dissociation barrier.[59] Another method by which the product may be formed is via an intramolecular rearrangement of the coordinated solvent molecule.[60,61] In paper I it was found that the ethyl-solvated dicarbonyls were stable to ∼180 ns and 6.8 μs for the Mn and Re systems, respectively. Given the trend of the strength of the metal alkane interactions, as well as the relatively long lifetimes of the ethyl adducts, the mechanism of product formation was described as dissociative. However, for the η^5-CpV(CO)$_3$ system, the reaction is almost complete on the ultrafast time scale. This is several orders of magnitude faster than what was observed for the d^6 Re and Mn dicarbonyl intermediates, despite the greater steric hindrance of the vanadium tricarbonyl species. This may be a consequence of a weaker V−alkane interaction, which allows a much faster dissociation time to form the final product. This is reasonable in light of the fact that η^5-CpV(CO)$_3$ is known to be more reactive than η^5-CpMn(CO)$_2$ and η^5-CpRe(CO)$_2$ in alkane solvents.[62] Unfortunately, our data do not allow us to rule out either an intramolecular or intermolecular rearrangement pathway for this reaction and we are presently working to determine the exact nature of this mechanism.

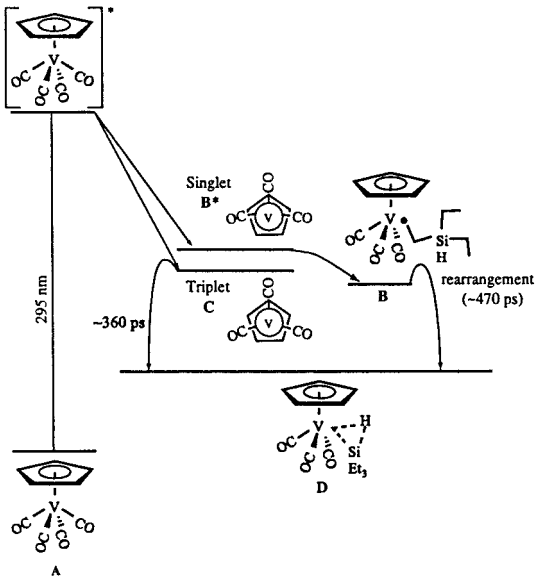

Figure 7. Proposed reaction mechanism for the silicon−hydrogen bond activation by η^5-CpV(CO)$_4$ covering the ultrafast dynamics to nanosecond kinetics. The nascent singlet η^5-CpV(CO)$_3$, denoted B*, is also shown for the purpose of discussion. See text for details.

Reaction Mechanism. In light of the above discussion, the photochemical Si−H bond activation reaction of η^5-CpV(CO)$_4$ in neat Et$_3$SiH under the ambient conditions is summarized in Figure 7. Excitation at 295 nm results in the generation of the tricarbonyl η^5-CpV(CO)$_3$ in either its electronic singlet or triplet manifold. Solvation of C via the Si−H bond leads to the final product D on a time scale of 360 ± 10 ps, possibly through a concerted coordination/spin crossover process. Solvation of B* through the ethyl group of the solvent molecule results in B, which decays to the product D on a time scale of 470 ± 75 ps.

V. Conclusion

The use of the femtosecond UV pump-IR probe spectroscopy allows the elementary reaction steps of photochemical Si−H bond activation, including changes in molecular conformation and electronic multiplicity, to be studied by monitoring the time evolution of the reactive intermediates. The nature of the

intermediates whose lifetimes were too short for conventional spectroscopic characterization were studied using quantum-chemical methods. We have investigated the photochemical Si−H bond activation reaction by group VB, d^4 transition metal complex η^5-CpV(CO)$_4$. The detailed reaction mechanism is summarized in Figure 7. We have shown in this paper that the reaction dynamics of η^5-CpV(CO)$_4$ and η^5-CpMn(CO)$_3$ with Et_3SiH have many similarities on the ultrafast time scale. For one, both form triplet species in geometries different from those of the singlet state following photolysis. The interconversion from the unsolvated triplets to solvated singlet species is likely to be a concerted solvation/spin crossover mechanism. This process is facilitated via solvation by the Si−H bond in triethylsilane. However, the formation of the product via rearrangement of the singlet ethyl-solvated η^5-CpV(CO)$_3$ was found be orders of magnitude faster than η^5-CpMn(CO)$_2$, indicative of the weaker alkane interaction or of a nondissociative mechanism being responsible for the formation of the product molecule.

Acknowledgment. This work was supported by a grant from the National Science Foundation. We also acknowledge equipment used under the Office of Basic Energy Science, Chemical Science Division, U.S. Department of Energy contract DE-AC03-76SF00098. We thank C. B. Moore for the use of the static FTIR spectrometer; A. P. Alivasatos for the use of a UV−vis spectrometer, and J. S. Yeston and P. J. Alaimo for assistance with handling of the samples. We would also like to acknowledge Prof. Kent R. Wilson for all of our conversations over the years, for his insight into many of our problems, and for his enthusiasm for ultrafast processes in chemistry and in general.

References and Notes

(1) Jetz, W.; Graham, W. A. G. *Inorg. Chem.* **1971**, *10*, 4.
(2) Bromberg, S. E.; Yang, H.; Asplund, M. C.; Lian, T.; McNamara, B. K.; Kotz, K. T.; Yeston, J. S.; Wilkens, M. J.; Frei, H.; Bergman, R. G.; Harris, C. B. *Science* **1997**, *278*, 260.
(3) Arndtsen, B. A.; Bergman, R. G.; Mobley, T. A.; Peterson, T. H. *Acc. Chem. Res.* **1995**, *28*, 154.
(4) Bergman, R. G. *Science* **1984**, *223*, 902.
(5) Schubert, U. *Adv. Organomet. Chem.* **1990**, *30*, 151.
(6) Yang, H.; Kotz, K. T.; Asplund, M. C.; Harris, C. B. *J. Am. Chem. Soc.* **1997**, *119*, 9564.
(7) Yang, H.; Asplund, M. C.; Kotz, K. T.; Wilkens, M. J.; Frei, H.; Harris, C. B. *J. Am. Chem. Soc.* **1998**, *120*, 10154.
(8) George, M. W.; Haward, M. T.; Hamley, P. A.; Hughes, C.; Johnson, F. P. A.; Popov, V. K.; Poliakoff, M. *J. Am. Chem. Soc.* **1993**, *115*, 2286.
(9) From ref 8, the CO absorption bands in the oxidative addition product CpV(CO)$_3$(HSiCl$_3$) are blue shifted with respect to the parent absorptions. The absorption bands of CpV(CO)$_3$(HSiEt$_3$), however, are red shifted, indicating an arrested oxidative addition of the metal center.
(10) Hitam, R. B.; Rest, A. J. *Organometallics* **1989**, *8*, 1598.
(11) Rest, A. J. *Organometallics* **1992**, *11*, 3646.
(12) Faber, G. C.; Anjelici, R. J. *Inorg. Chem.* **1970**, *9*, 1587.
(13) Alway, D. G.; Barnett, K. W. *Inorg. Chem.* **1980**, *19*, 779.
(14) Faber, G. C.; Angelici, R. J. *Inorg. Chem.* **1984**, *23*, 4871.
(15) Kowaleski, R. M.; Kipp, D. O.; Stauffer, K. J.; Swepston, P. N.; Basolo, F. *Inorg. Chem.* **1985**, *24*, 3750.
(16) Freeman, J. W.; Basolo, F. *Organometallics* **1991**, *10*, 256.
(17) Lian, T.; Bromberg, S. E.; Asplund, M. C.; Yang, H.; Harris, C. B. *J. Phys. Chem.* **1996**, *100*, 11994.
(18) Bethune, D. S. *Appl. Opt.* **1981**, *20*, 1987.
(19) Becke, A. D. *J. Chem. Phys* **1993**, *98*, 5648.
(20) Lee, C.; Yang, W.; Parr, R. G. *Phys. Rev.* **1988**, *B41*, 785.
(21) Stephens, P. J.; Devlin, F. J.; Chabalowski, C. F.; Frisch, M. J. *J. Phys. Chem.* **1994**, *98*, 11623.
(22) Hehre, W. J.; Ditchfield, R.; Pople, J. A. *J. Chem. Phys.* **1972**, *56*, 2257.
(23) Francl, M. M.; Petro, W. J.; Hehre, W. J.; Binkley, J. S.; Gordon, M. S.; Defrees, D. J.; Pople, J. A. *J. Chem. Phys.* **1982**, *77*, 3654.
(24) Hay, P. J.; Wadt, W. R. *J. Chem. Phys.* **1985**, *82*, 299.
(25) Jaguar 3.5; Schrodinger, Inc.: Portland, OR, 1998.
(26) Schmidt, M. W.; Baldridge, K. K.; Boatz, J. A.; Elbert, S. T.; Gordon, M. S.; Jensen, J. H.; Koseki, S.; Matsunaga, N.; Nguyes, K. A.; Su, S.; Windus, T. L.; Dupuis, M.; Montgomery, J. A. *J. Comput. Chem.* **1993**, *14*, 1347.
(27) Gledening, E. D.; Badenhoop, J. K.; Reed, A. E.; Carpenter, J. E.; Weinhold, F. *NBO 4.0*; Theoretical Chemistry Institute, University of Wisconson, Madison:, 1996.
(28) Dunning, T. H. J.; Hay, P. J. *Methods of Electronic Structure Theory*; Plenum: New York, 1977; Vol. 2.
(29) Hay, P. T.; Wadt, W. R. *J. Chem. Phys* **1985**, *82*, 270.
(30) Hay, P. J.; Wadt, W. R. *J. Chem. Phys* **1985**, *82*, 284.
(31) Nakano, H. *J. Chem. Phys.* **1993**, *99*, 7983−7992.
(32) Liu, B.; McLean, A. D. *J. Chem. Phys.* **1973**, *59*, 4557.
(33) Xantheas, S. *J. Chem. Phys.* **1996**, *104*, 8821.
(34) Dougherty, T. P.; Heilweil, E. J. *Chem. Phys. Lett.* **1994**, *227*, 19.
(35) Dougherty, T. P.; Grubbs, W. T.; Heilweil, E. J. *J. Phys. Chem.* **1994**, *98*, 9396.
(36) Dougherty, T. P.; Heilweil, E. J. *J. Phys. Chem.* **1996**, *100*, 201.
(37) Uncertainties represent one standard deviation.
(38) While the parent bleach kinetics are obscured at early times, there is no observed recovery of the parent after 20 ps.
(39) Bode, B. M.; Gordon, M. S. *J. Mol. Graphics Mod.* **1998**, *16*, 133−138.
(40) Almond, M. J.; Page, E. M.; Rice, D. A.; Hagen, K. *J. Organomet. Chem.* **1996**, *511*, 303.
(41) For example, it is known that the CpRe(CO)$_3$(*n*-heptane) complex is much more stable than CpV(CO)$_3$(*n*-heptane) by its longer lifetime.[62] Consequently, in paper I the calculated C−H bond length of ethane increase by +0.07 Å when coordinated to the Rhenium complex, compared to our calculated value of +0.02 Å.
(42) Knorr, M.; Muller, J.; Schubert, U. *Chem. Ber., 120*, 879.
(43) Siegbahn, P. E. M. *J. Am. Chem. Soc.* **1996**, *118*, 1487.
(44) Smith, K. M.; Poli, R.; Lagzdins, P. *Chem. Eur. J.* **1999**, *5*, 1598.
(45) Ishikawa, Y.; Brown, C. E.; Hackett, P. A.; Rayner, D. M. *Chem. Phys. Lett.* **1988**, *150*, 506.
(46) Brown, C. E.; Ishikawa, Y.; Hackett, P. A.; Rayner, D. M. *J. Am. Chem. Soc.* **1990**, *112*, 2530.
(47) Zaric, S.; Hall, M. B. *J. Phys. Chem.* **1997**, *101*, 4646.
(48) Teuben, J. N.; Huffman, J. C.; Caulton, K. G. *J. Organomet. Chem.* **1983**, *255*, 193.
(49) Hessen, B.; Meetsma, A.; Teuben, J. H. *J. Am. Chem. Soc.* **1988**, *110*, 4860.
(50) Jonas, V.; Theil, W. *J. Chem. Phys.* **1996**, *105*, 3636.
(51) Zaric, S.; Couty, M.; Hall, M. B. *J. Am. Chem. Soc.* **1997**, *119*, 2885.
(52) Zaric, S.; Hall, M. B. *J. Phys. Chem.* **1998**, *102*, 1963.
(53) In the CH_4 matrix study, the intermediate observed at 2020 cm^{-1} also absorbs at 1928 cm^{-1}, which is only 3 cm^{-1} red shifted from the parent band.
(54) Blomberg, M. R. A.; Siegbahn, P. E. M.; Svensson, M. *J. Am. Chem. Soc.* **1992**, *114*, 6095.
(55) Siegbahn, P. E. M.; Svensson, M. J. *J. Am. Chem. Soc.* **1994**, *116*, 10124.
(56) Carroll, J. J.; Weisshaar, J. C.; Haug, K. L.; Blomberg, M. R. A.; Siegbahn, P. E. M.; Svensson, M. *J. Phys. Chem.* **1995**, *99*, 13955.
(57) Bengali, A. A.; Bergman, R. G.; Moore, C. B. *J. Am. Chem. Soc.* **1995**, *117*, 3879.
(58) Dougherty, T. P.; Heilweil, E. J. *J. Chem. Phys.* **1994**, *100*, 4006.
(59) Ladogana, S.; Nayak, S. K.; Smit, J. P.; Dobson, G. R. *Inorg. Chem.* **1997**, *36*, 650.
(60) Xie, X.; Simon, J. D. *J. Am. Chem. Soc.* **1990**, *112*, 1130.
(61) O'Driscoll, E.; Simon, J. D. *J. Am. Chem. Soc.* **1990**, *112*, 6580.
(62) Sun, X. Z.; Grills, D. C.; Nikiforov, S. N.; Poliakoff, M.; George, M. *J. Am. Chem. Soc.* **1997**, *119*, 7521.